Proc. JCF11-11, pp. 59 – 69 (2011)

Localization of Nuclear Reactions in the Cold Fusion Phenomenon

Hideo Kozima
Cold Fusion Research Laboratory,
597-16 Yatsu, Aoi, Shizuoka, Shizuoka 421-1202, Japan

Abstract

One of the characteristics of the cold fusion phenomenon (CFP), i.e. low energy nuclear reactions in solids with high density hydrogen isotopes at near room-temperature in ambient radiations, is the localization of nuclear reactions relevant to the phenomenon. The earliest data sets showing the localization of nuclear reactions were given by Iyengar and Srinivasan (1989, 1990) for product tritium localized in spots (fraction of a millimeter or less in size) at surfaces of a Ti sample. Morrey et al. (1990) reported $^{4}_{2}$He in surface layers of Pd with a width of about 25 μm. Okamoto et al. (1994) observed nuclear transmutation of minor elements in surface layers of Pd samples, especially $^{27}_{13}$Al into $^{28}_{14}$Si, in a layer of about 2 μm. Miley et al. (1996) observed various transmutation products, especially transmutation of $^{A}_{28}$Ni isotopes, in the thin Ni layer of width about 0.1 μm in a protium system. Mizuno et al. (1996) also observed similar nuclear transmutations in PdD_x and AuH_x systems. Iwamura et al. (2002, 2005) observed transmutations of Sr, Cs and Ba into Mo, Pr and Sm, respectively, in/on a Pd surface layer of thickness about 100 A. Furthermore, the second product confirmed its spatial localization with a diametrical size of about 100 μm. Thus, we know that the reaction products of the CFP are localized in regions at surface layers about a few μm in width of massive CF materials and also in thin CF materials with layer structures of widths less than one μm.

The confinement of nuclear reactions in surface/boundary layers of a few μm might be a characteristic of the CFP in protium and deuterium systems. This characteristic of the CFP is explained by the structure of a CF material composed of (1) a host material composed of a metal and a hydrogen isotope and (2) a guest material including agents for the CFP on the surface of the former. The localization of nuclear reactions in the guest material in spot-like regions is another characteristic showing nuclear reactions between the agent (such specific nuclei as alien nuclei (Li, Sr, Cs) or the irregularity of atomic arrays). These characteristics of localized nuclear reactions are investigated quantum mechanically using properties of nucleus and proton/deuteron wavefunctions

in the CF material.

1. Introduction

To make people recognize importance of the controversial research fields like the cold fusion phenomenon that they have not known well about the details of experimental data in it, it is necessary to arrange experimental data sets along lines easy to understand the complexity of the data. One of characteristics of the cold fusion phenomenon (CFP), i.e. phenomenon composed of nuclear reactions in complex solid materials containing a lot of hydrogen isotopes in a non-equilibrium condition including ambient radiations, is the localization of reactions revealed by transmuted nuclei in surface or boundary layers with a width of about a few micrometer (1 μm = 10^{-4} cm). The localization of the transmuted nuclei is one of the direct evidences of nuclear reactions in the CFP ([1.1], Section 2.2.1.1). If we are able to understand the cause of this localization in terms of common senses of the modern science, it is helpful to make the phenomenon recognized as an object of science and also to investigate the CFP as a part of modern science in interdisciplinary field among nuclear physics, solid-state physics and catalytic chemistry.

There are many experimental data sets showing the surface nature of nuclear reactions in the CFP observed from the year of 1989 and increasing the number and accuracy of measurements until now. The first confirmation of the locality of the phenomenon may be the paper by Morrey et al. [1.2] observing He atoms in the surface layer of width about 25μm of the Pd sample in which excess heat was observed. Iyengar and Srinivasan et al. [1.3, 1.4] observed tritium localized in spots (fraction of a millimeter or less in size) at surfaces of Ti samples. Following these pioneering works, there have reported various data sets showing localization of nuclear products in surface layers of massive CF materials [1.5 – 1.15] and also in several layer structures with width less than 1 μm [1.16 – 1.29].

The localization of nuclear products should be investigated as it is and also in relation to other events in the CFP to clarify the mechanisms realizing the wonderful events of the CFP.

In this paper, we give an approach to the unified explanation of the localization of nuclear emission sources, $^{4}_{2}$He generation and nuclear transmutations in the CFP using a phenomenological model and a quantal approach to the mechanism of nuclear reactions in CF materials.

2. The TNCF Model and Experimental Data Sets

The trapped neutron catalyzed fusion (TNCF) model proposed by us [2.1] and extended later to explain nuclear transmutations with the large changes of mass and proton numbers [1.1] is used to explain nuclear transmutations observed in localized regions in this section. From experimental facts, we assume materials where occurs the cold fusion phenomenon (CFP) are divided into two regions. (1) The first is the **host material** composed of interlaced lattices of (a) Pd, Ti, Ni, C, or several other elements and (b) protium or deuterium. (2) The second is the **guest material** composed of elements placed in the surface or boundary regions of the host material with different regularity from the first.

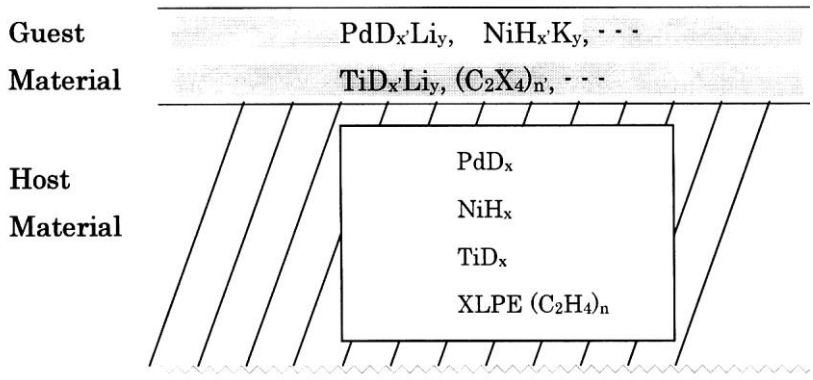

Fig. 2.1 Host and guest materials in the cold fusion material

The key assumption of the model is the existence of the so-called trapped neutrons in the host material in a neutron band. The **neutron Bloch waves** in the band are reflected at the boundary of the host and guest materials making accumulation of Bloch waves. The accumulation makes the density of the trapped neutron at the boundary region very high as $10^{8} – 10^{11}$ cm $^{-3}$.

The model assumes three types of nuclear reactions between the trapped neutron and a nucleus ${}^{A}_{Z}X$ placed in the guest material out of phase of the lattice of the host material:

1. Absorption of single neutron by a nucleus ${}^{A}_{Z}X$ followed by a disintegration of ${}^{A+1}_{Z}X^{*}$;
   $n + {}^{A}_{Z}X = {}^{A+1}_{Z}X^{*} \rightarrow$ (to succeeding nuclear processes) (1.1)
2. Absorption of a neutron-proton cluster ${}^{A}_{Z}\delta$ by a nucleus ${}^{A'}_{Z'}X$:
   ${}^{A}_{Z}\delta + {}^{A'}_{Z'}X = {}^{A+A'}_{Z+Z'}X^{*} \rightarrow$ (to succeeding nuclear processes) (1.2)
3. Nuclear interaction between a neutron drop ${}^{A}_{Z}\Delta$ and a nucleus ${}^{A'}_{Z'}X$:
   ${}^{A}_{Z}\Delta + {}^{A'}_{Z'}X = {}^{A+A'-a}_{Z+Z'-b}\Delta + {}^{A+A'+a}_{Z+Z'+b}X^{*} \rightarrow$ (to succeeding nuclear processes). (1.3)

The neutron cluster ${}^{A}_{Z}\delta$ and neutron drop ${}^{A}_{Z}\Delta$ are assumed to be composed of Z protons and (A - Z) neutrons. The difference is only the number of nucleons in them; A is

supposed to be less than 10 in the cluster and larger than or equal to 10 in the drop.

2.1 Data by Morrey et al. [1.2]

The first evidence of locality of nuclear reactions was observed by Morrey et al. [1.2] when they tried to check generation of $^4_2$He in PdD_x samples that had shown excess heat by Fleischmann et al. [2.2]. They have observed $^4_2$He in the surface layer of width 40 μm of the sample with an amount incompatible with the excess heat reportedly observed in the same sample. The discrepancy was resolved by our consideration of the mechanism catalyzed by a trapped neutron between $^6_3$Li nucleus at the surface producing excess heat and $^4_2$He by a phenomenological model [2.2, Section 11.8].

2.2 Data obtained in BARC (Bhabha Atomic Research Center) in India [1.3, 1.4]

Localization of tritium in TiD_x was observed by a group in BARC (Bhabha Atomic Research Center) in India [1.3, 1.4] (Fig. 2.2). They concluded that tritium is invariably concentrated in highly localized spots (fraction of a millimeter or less in size) each containing typically about 10^{12} to 10^{14} atoms (2 to 200 kBq) of tritium. In addition to the localization of the product tritium, they observed a high ratio N_t/N_n of tritium to neutron as $10^6 - 10^9$ ($N_t/N_n|_{ex} \sim 10^6 - 10^9$).

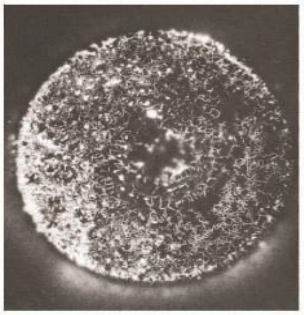

Fig. 2.2 Autoradiograph of central Ti electrode of PF (plasma focus) device (5 weeks after charging) [1.3]

The large imbalance in production rates of tritium and neutron has been explained by a mechanism occurring in the CF material by the TNCF model [1.1, 2.2, 2.3] which predicts the ratio of about 10^7 ($N_t/N_n|_{th} \sim 10^7$).

2.3 Data by Dash et al. [1.5, 1.6]

Surface morphology and change of elements in the surface layer of PdD_x samples have been investigated by Dash et al. (Fig. 2.3).

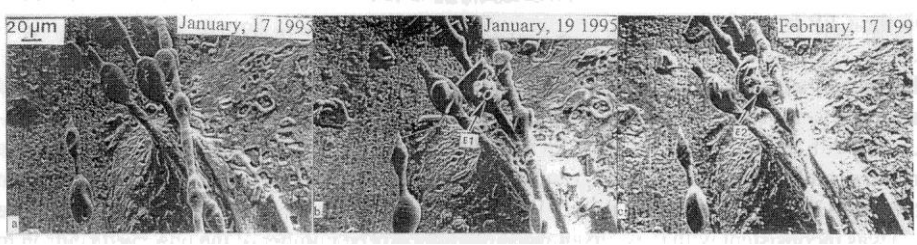

Fig. 2.3 Surface morphology of PdD_x [1.5]

The changes of isotope ratios of Ti and Pd observed by them have been qualitatively explained by the TNCF model ([1.1] Appendix C7, [2.4]). The cause of high temperature at the surface region resulting in the complex morphology observed by Dash et al. has been investigated using the TNCF model. The same investigation will be applied to the hot spots containing tritium about 10^{12} to 10^{14} atoms observed by Iyengar et al [1.3].

It is interesting to note their result [1.6] that the excess heat generation does not occur when H_2SO_4 is replaced by D_2SO_4 in the $Pd/D_2O + H_2SO_4$ system. This point will be discussed elsewhere [2.5].

2.4. Data by Okamoto et al. [1.7]

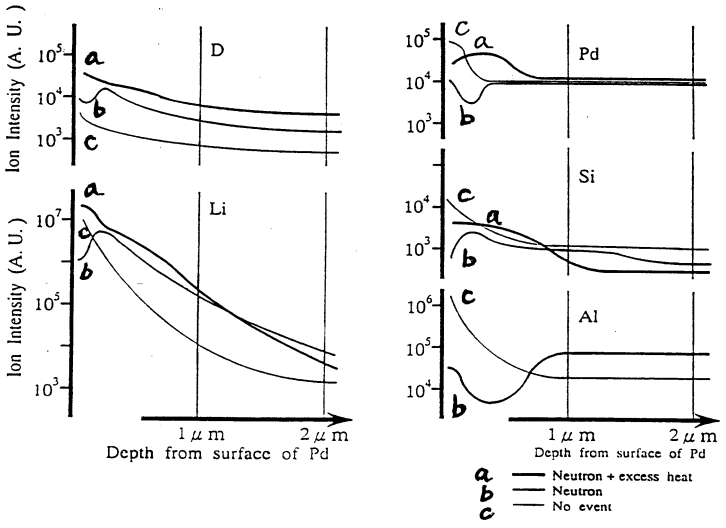

Fig. 2.4 Depth profile of D, Li, Pd, Si and Al observed by Okamoto et al. [1.7]

The data by Okamoto et al. (Fig. 2.4) obtained in a Pd/D_2O+LiOD/Pt system was successfully analyzed by the single neutron absorption mechanism of the TNCF model. The result explains the observed decrease of Al and increase of Si by the following

reactions;

$$n + {}^{27}_{13}\mathrm{Al} = {}^{28}_{13}\mathrm{Al}^* = {}^{28}_{14}\mathrm{Si} + e^- + \underline{\nu}_e, \quad (2.4)$$

where $\underline{\nu}_e$ is the electron neutrino.

2.5. Data by Miley et al. [1.16, 1.17]

The data of nuclear transmutation observed by Miley et al. [1.16, 1.17] in beads (microspheres) of polystyrene core plated with thin (~ 1 μ m) metal films of Cu, Ni and/or Pd on the surface [1.18] (Fig. 2.5) were analyzed by the TNCF model with a single neutron absorption followed by a decay depending on the intermediate excited nucleus:

- $n + {}^{A}_{Z}\mathrm{Ni} = {}^{A+1}_{Z}\mathrm{Ni}^* \rightarrow (\gamma, \beta, \alpha\text{-decays})$. (2.5)

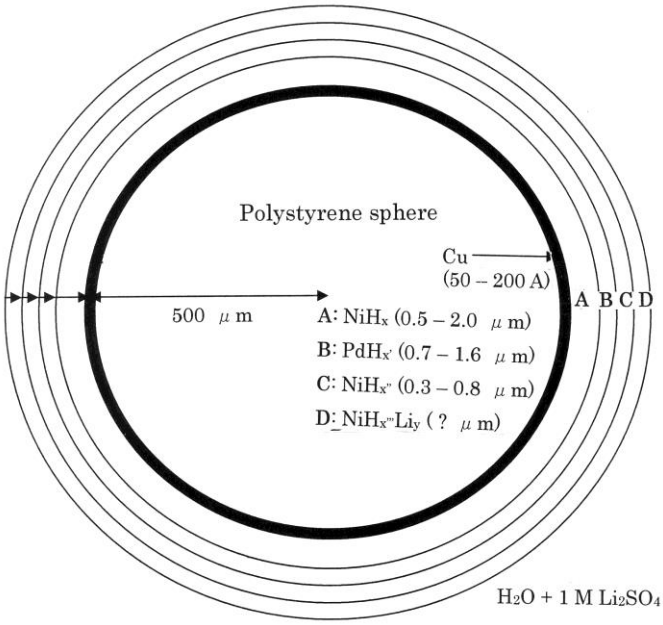

Fig. 2.5 Patterson Bead (Schematic illustration) used with H_2O + 1 M Li_2SO_4 electrolyte.

The resultant ratio of nickel isotopes ${}^{A}_{Z}\mathrm{Ni}$ (A = 59, 63 and 65) is compared with the experimental result as follows:

- $(N_{59}: N_{63}: N_{65})_{ex} = 1 : 0.27 : 0.12$. (2.6)
- $(N_{59}: N_{63}: N_{65})_{th} = 1 : 0.17 : 5.73 \times 10^{-3}$. (2.7)

On the other hand, the excess heat expected from the assumed nuclear reactions is compared with the experimental result assuming that the liberated energy was totally thermalized in the system;

- $P_{ex} = 0.5 \pm 0.4$ W. (2.8)
- $P_{th} = 0.12$ W. (2.9)

We may conclude that the coincidence of the theoretical and the experimental results is fairly good.

The other various products such as Fe, Si, Mg, Cu, Cr, Zn, and Ag should be explained by the use of the reactions (2.3) catalyzed by neutron drops. Some of these cases are given in the next subsection.

2.6 Data by Mizuno et al. [1.9 – 1.12]

Mizuno et al. and Ohmori et al. have made various excellent experiments on the protium and deuterium systems with Au, W, Pt, Pd and Ni cathodes and have reported the results in many papers including ones cited in this paper [1.9 – 1.12]. Localization of nuclear transmutation products at surface regions has been determined in addition to the change of surface morphology shown in Fig. 2.6 (Morphology change in AuH_x system).

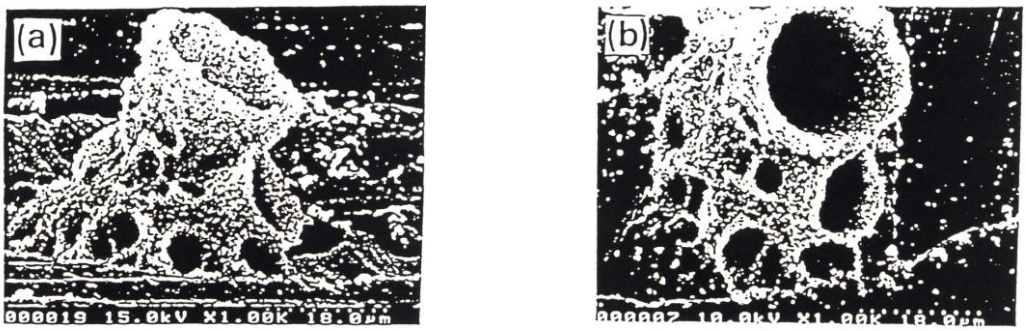

Fig. 2.6 SEM images of the Au electrode after the electrolysis in 0.5 M Na_2CO_3 + H_2O for 30 days at a current density of 500 mA/cm^3, (a) image from upside (× 1,000), (b) image from horizontal side (× 1,000) [1.11].

From their figures showing profiles of newly generated elements in PdD_x system, we cite here those for isotopes of chromium (Cr) in Fig. 2.7 [1.10].

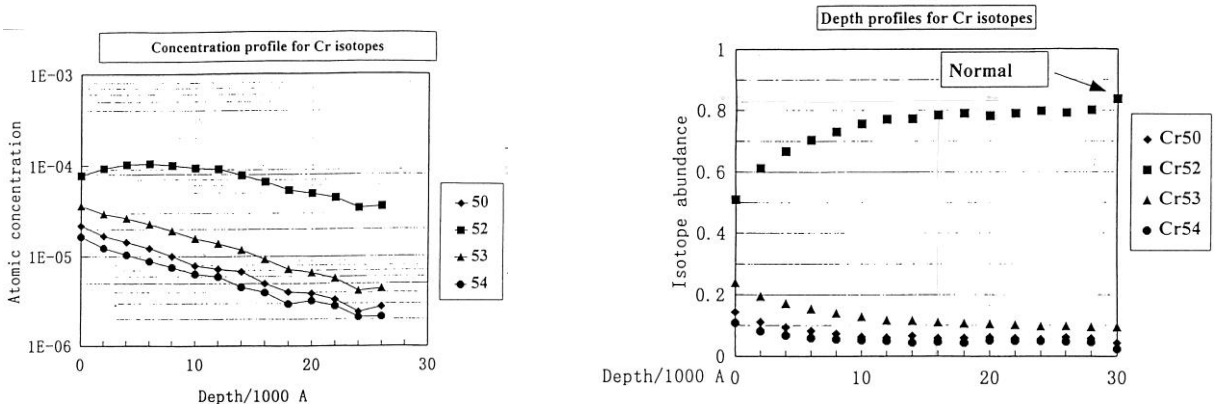

Fig. 2.7 Isotopes of ${}^{A}{}_{24}Cr$ (A = 50, 52, 53 and 54) in the surface region showing variation of concentration and isotopic ratios in depth from the surface [1.10].

The elements produced in the surface region of Pd samples includes light nuclei (O, C, Ca, Na, Mg and Al) and heavy nuclei (Cr, Fe, Cu, Zn, Br, Xe, Cd, Hf, Re, Pt, Ir and Hg) the shifts of isotopic abundances from natural ones are small in the former and large in the latter.

A possible explanation of the reactions to generate those various elements, especially the heavy nuclei, is given by the nuclear reactions (2.3) catalyzed by the neutron drops ${}^{A}{}_{Z}\Delta$. An example of possible nuclear reactions mediated by the neutron drops ${}^{A}{}_{Z}\Delta$ in the cf-matter formed at around surface region are written down as follows (α = 190 – 198);

$${}^{\alpha}{}_{78}Pd + {}^{A}{}_{Z}\Delta = {}^{\alpha'}{}_{24}Cr + {}^{\alpha''}{}_{26}Fe + {}^{\alpha'''}{}_{29}Cu + {}^{\alpha''''}{}_{30}Ni + {}^{A'}{}_{Z'}\Delta \qquad (2.10)$$

when $\alpha = 102 - 110$, $\alpha + A = \alpha' + \alpha'' + \alpha''' + \alpha'''' + A'$, $78 + Z = 24 + 26 + 29 + 30 + Z'$.

Another possible reaction may be that with two neutron drops as follows;

$${}^{\alpha}{}_{78}Pd + {}^{A}{}_{Z}\Delta + {}^{A'}{}_{Z'}\Delta = {}^{\alpha'}{}_{24}Cr + {}^{\alpha''}{}_{26}Fe + {}^{\alpha'''}{}_{29}Cu + {}^{\alpha''''}{}_{30}Ni + {}^{A''}{}_{Z''}\Delta \qquad (2.11)$$

with $\alpha + A + A' = \alpha' + \alpha'' + \alpha''' + \alpha'''' + A''$, $78 + Z + Z' = 24 + 26 + 29 + 30 + Z''$.

2.7 Data by Qiao et al. [1.13]

Qiao et al. [1.13] made an experiment of excess heat and nuclear transmutation on a Pd wire with a diameter 340 μm deuterated by the gas contact method. After one year of loading and de-loading process, they measured the element composition of the sample at six points depicted in Fig. 2.8.

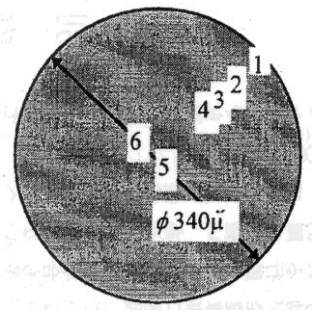

Fig. 2.8 Cross-section of the Pd wire sample indicating points where analyzed element composition.

The experimental result of the atomic concentration is given in Table 2.1

	Atomic Concentration (%)					
Elements	Point 1	Point 2	Point 3	Point 4	Point 5	Point 6
Pd	57.66	58.24	58.62	59.38	99.14	98.96
Zn	41.40	40.84	40.49	39.85	0.42	0.71
Pb	0.82	0.90	0.83	0.75	0.12	0.05
Fe	0.06	0.03	0.07	0.02	0.16	0.19
Cu	0.04	0.00	0.00	0.00	0.08	0.09
Sr	0.00	0.00	0.00	0.00	0.08	0.00

Table 2.1 Elements composition of reacted Pd (cross section)

In this table, we take up only the data of Zn and analyze them by the NT by the single neutron absorption followed by fission. The probable reaction inducing the transmutation of Pd into Zn is written down as follows assuming a fission reaction:

$$n + {}^{A}_{46}\mathrm{Pd} \rightarrow {}^{A+1}_{46}\mathrm{Pd}^{*} \rightarrow {}^{A'}_{30}\mathrm{Zn} + {}^{A+1-A'}_{16}\mathrm{S}, \tag{2.12}$$

with $A = 102 - 110$ and $A' = 64 - 70$ for stable isotopes and therefore

$$A + 1 - A' \equiv A'' \geq 33. \tag{2.13}$$

The cross section σ for the absorption reaction in the above reaction ranges from 0.2 to 20 barns; σ = 3.36, 0.52, 20.25, 0.30, 8.50 and 0.23 barns for A = 102, 104, 105, 106, 108 and 110, respectively. Assuming the intermediate nucleus ${}^{A+1}_{46}\mathrm{Pd}^{*}$ in the above reaction is unstable and decays by and by into Zn and S, we can calculate the number of Zn atoms N_{Zn} generated in a time τ as a function of the density of the trapped neutron n_{n} by the following relation according to our recipe of our model [1.1, 2.2, 2.3]:

$$N_{\mathrm{Zn}} = 0.35\, n_{\mathrm{n}}\, v_{\mathrm{n}}\, n_{\mathrm{Pd}}\, V\, \tau\, \Sigma 0.01 p_A \sigma_A \xi, \tag{2.14}$$

where v_{n} is the thermal velocity of the trapped neutron, n_{Pd} is the density of palladium, p_A (in %) is the natural abundance of a Pd isotope with mass number A, σ_A is the absorption cross section of the above reaction for a mass number A, ξ is a numerical factor arbitrarily introduced into the theory to express the degree of instability (or reactivity) of the trapped neutron and is assumed to be 1 in the boundary region (and 0.1 in the volume), and V is the volume of the sample.

Using an average value $N_{\mathrm{Zn}} = 4.065 \times 10^{-3}\, n_{\mathrm{Pd}}\, V$ of the experimental data at Points 1 to 4 generated in τ = 1 y (= 3.15×10^{7} s) and $V = (1.7^2 - 1.3^2) \times 10^{-4}$ cm^3 = 1.2×10^{-4} cm^3 per unit length of the Pd wire, we obtain the parameter n_{n} as follows (ξ = 1 is assumed);

$$n_{\mathrm{n}} = 9.9 \times 10^{8} \ \mathrm{cm}^{-3}, \tag{2.15}$$

which is in the lower range of values determined for other experimental data sets [2.1].

Many of the isotopes of sulfur (S) generated finally in the above reaction have β-decay modes and generate chlorine (Cl) or finally argon (Ar) which are gaseous and

not expected to remain in the sample to be detected there.

The excess heat accompanied with the fission generating Zn is estimated taking only the predominant modes in the above reaction and is $Q_{th} \approx 0.5$ W. This value of excess heat is compared with the value $Q_{ex} = 0.82$ W obtained by them (cf. [2.1] Section 11.12d, [2.6]).

2.8 Data by Campali et al. [1.14, 1.15]

Campali et al. [1.14, 1.15] investigated photon and particle emission, heat production and surface transmutation in the Ni-H system loaded by gas contact with cylindrical and planar samples of pure Ni and Ni alloy ($Ni_{7.6}Cr_{20.6}Fe_{70.4}Mn_{1.4}$). Their results give us another interesting example of the CFP in protium systems with identification of the place where occur nuclear reactions resulting in transmutations at the sample surface.

New elements between C and Zn were observed after same months of heat production, the concentrations of which depended on the position. One example of elemental analysis of the sample observed at a point is given in Fig. 2.9.

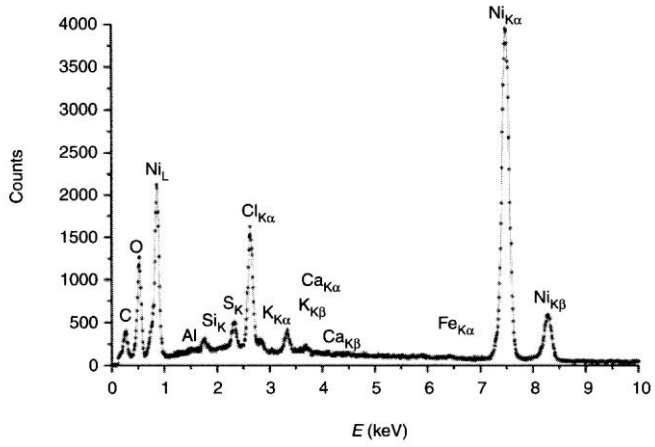

Fig. 2.9 Example of elemental analysis of the Ni sample. (At a point on the cylindrical rod sample with a length 9.0 cm.)

The concentrations of the new elements Cu and Zn varied along the rod surface of the Ni alloy sample as shown in Fig. 2.10.

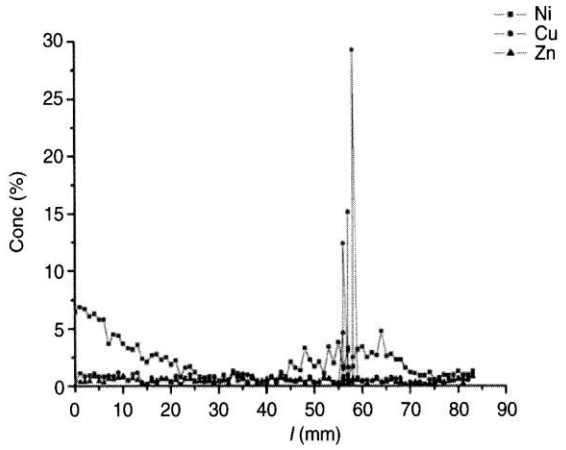

Fig. 2.10 Spatial distribution (along the rod) of Ni, Cu and Zn on the sample surface of Ni alloy ($Ni_{7.6}Cr_{20.6}Fe_{70.4}Mn_{1.4}$).

The mechanism of Cu and Zn formation in this case may be the single neutron and neutron-proton cluster absorptions followed by decay processes. Several examples of the reaction are written down as follows [1.1 (Section 2.5), 2.1 (Section 11.11)];

$$n + {}^{62}_{28}\mathrm{Ni} = {}^{63}_{28}\mathrm{Ni}^{*} \rightarrow {}^{63}_{29}\mathrm{Cu} + e^{-} + \underline{\nu}_e, \quad (2.16)$$

$$n + {}^{64}_{28}\mathrm{Ni} = {}^{65}_{28}\mathrm{Ni}^{*} \rightarrow {}^{65}_{29}\mathrm{Cu} + e^{-} + \underline{\nu}_e, \quad (2.17)$$

$${}^{6}_{3}\delta + {}^{57}_{26}\mathrm{Fe} = {}^{63}_{29}\mathrm{Cu}^{*} \rightarrow {}^{63}_{29}\mathrm{Cu} + \gamma, \quad (2.18)$$

$${}^{8}_{4}\delta + {}^{56}_{26}\mathrm{Fe} = {}^{64}_{30}\mathrm{Zn}^{*} \rightarrow {}^{64}_{30}\mathrm{Zn} + \gamma. \quad (2.19)$$

2.9 Data by Iwamura et al. [1.19 – 1.23]

The interesting experimental data sets obtained by Iwamura et al. [1.19 – 1.23] give us information about the local nature of the nuclear transmutation and also a phase of neutron-nucleus interactions in the CFP, the absorption of a neutron-proton cluster by a nucleus. They used a specific structure called "Pd complex" shown in Fig. 2.11.

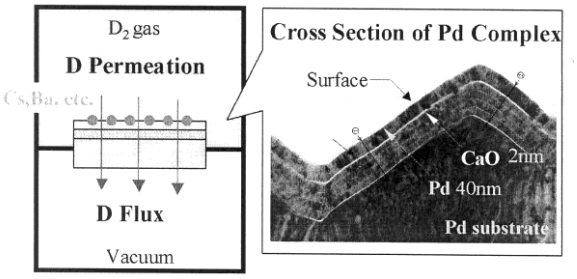

Fig. 2.11 Pd complex used in the experiments by Iwamura et al. [1.23]

After adding alien elements Cs, Sr or Ba on the surface, D_2 gas was permeated through this structure as shown in Fig. 2.11, they investigated the surface of the

complex and found nuclear transmutations of elements Cs to Pr, Sr to Mo and $^{A}_{56}$Ba to $^{A+12}_{62}$Sm. This results have clearly demonstrated the nuclear reactions catalyzed by neutron-proton clusters $^{8}_{4}\delta$ and $^{12}_{6}\delta$ that were already assumed before to explain nuclear transmutations (NTs) observed in deuterium and protium systems [1.2, 2.1];

- $^{A'}_{4}\delta + {}^{A}_{38}\mathrm{Sr} = {}^{A+A'}_{42}\mathrm{Mo}$,

  (A = 84, 86-88; A+A' = 92, 94 – 98, 100; A' = 4 – 16) (2.20)

  $^{8}_{4}\delta + {}^{133}_{55}\mathrm{Cs} = {}^{141}_{59}\mathrm{Pr}$, (2.21)

  $^{A'}_{6}\delta + {}^{A}_{56}\mathrm{Ba} = {}^{A+A'}_{62}\mathrm{Sm}$,

  (*A* = 132, 134 –138, A+ A' = 144, 147 – 150, 152, 154; A' = 6 – 22) (2.22)

In the case of the third reaction (2.22), they confirmed the transmutation from $^{137}_{56}$Ba and $^{138}_{56}$Ba to $^{149}_{62}$Sm and $^{150}_{62}$Sm, respectively [1.22]. These cases are explained by the reaction associated with the neutron drop $^{12}_{6}\delta$.

In addition to the data of nuclear transmutations catalyzed by the $^{A}_{Z}\delta$, they determined the locality of the positions where occur these NTs to generate Pr, Mo and Sm by using 100- and 500-micron x-ray beams (Fig. 2.12).

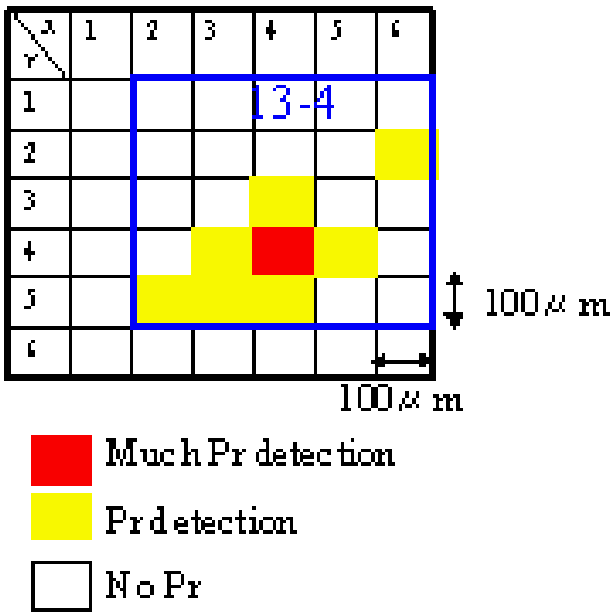

Fig. 2.12 Surface distribution of Pr for FG2 using 500-micron and 100-micron x-ray beams, mapping of Pr by 100-micron beam [1.23].

The localization of the nuclear transmutation confirmed in this experiment reminds us the localization of tritium observed by Iyengar et al. [1.3]. These localizations of nuclear products may be explained by the positive feedback mechanism described in our paper on the complexity [1.24] occurring in this case in localized regions.

In conclusion, their extensive data sets determined the localization of nuclear

reactions resulting in the NTs at hot spots with a diameter up to 10 to 50 nm (100 to 500 A) in the surface layer of thickness up to 10 nm (100 A).

2.10 Data by Szpak et al. [1.25 – 1.28]

Szpak et al. used a specific sample of the co-deposited Pd/D films on Au foils and Ni screens to observe the CFP with CR-39 and other techniques. Spectacular results obtained by them include localization of the heat sources in close proximity to the electrode-solution contact surface, occurrence of pits, or localized "hot spots," change of surface morphology (cauliflower, dendrite, and fractal), nuclear transmutations generating Al, Mg, Ca, Si, Zn and so on, generation of tritium, emission of energetic particles including neutrons with energies up to about 10 MeV. Also, they observed effects of static electric field on the excess heat and morphology change. It is interesting that their confirmation of a positive of protium in the Pd system but is less effective than deuterium for the CFP in pits formation. Similar difference between H and D in the Pd system is also observed by Celani et al. [2.7].

The emission of neutrons with energies about 10 MeV is analyzed in the paper presented at JCF11 [2.8].

2.11 Data by Celani et al. [1.29]

Celani et al. have done experiments with new type samples of Pd and Ni wire coated with thin multilayer nano-materials and treated in D_2 and H_2 gas with sample temperature up to 900 C. In the case of Ni wire [1.29], they observed change of surface morphology (Fig. 2.13) and changes of amounts (Ti, Cr, Co, As, Ir, Ti are increased and Sr, Pd are decreased) and changes of isotope ratios of Pd and B ($^{105}_{46}$Pd and $^{10}_{5}$B/$^{11}_{5}$B ratio decreased) while the amounts of Fe and Ni are constant.

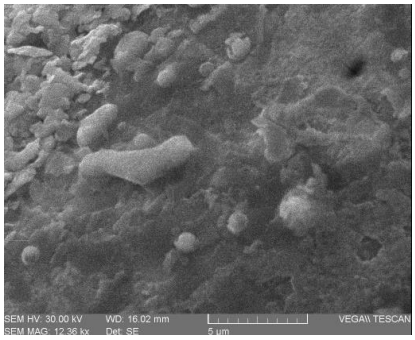

Fig. 2.13 Ni coated after gas treatment.

They observed a general tendency for the decrease of concentrations of isotopes that the smaller the mass number of the isotope, the larger the decrease of its concentration.

This tendency seems to show the nuclear transmutation (NT) by the single neutron absorption (2.1).

This mechanism for the NT is also useful to understand the remarkable decreases of $^{105}_{46}$Pd and $^{10}_{5}$B/$^{11}_{5}$B ratio if we consider the large cross-sections for thermal neutron absorption of $^{105}_{46}$Pd and $^{10}_{5}$B compared to other isotopes (20.25 and 3837 b, respectively). The increase of As may be the result of NT (2.2) by an absorption of $^{4}_{2}\delta$ by $^{31}_{71}$Ga while the decrease of the latter is not certain by their data. Reactions of this type have been used in Section 2.8 to explain the data by Campali et al. and confirmed by Iwamura et al. [1.20] already.

Their results have shown that the Ni-H system generate excess heat as well as the Pd-D system they used before confirming the long-lasted experience of Focardi et al. [2.9, 2.10].

3. Discussion and Conclusions

As we have shown above that the locality of the CFP is fairly common in protium and deuterium systems, it is necessary to explain it from unified point of view applicable to the both systems. The TNCF model proposed by us [1.1, 2.2 – 2.8] has given qualitative explanation of several data sets some of which are explained in Section 2. It means that the model may contain essentials of physics of nuclear reactions resulting in the CFP.

The local nature of the reaction in the CFP at the surface regions with a depth of about one micrometer (μm) may be explained by the accumulation of neutron Bloch waves and formation of the cf-matter at surfaces elaborated to justify the foundation of the model (cf. e.g. [1.1] Section 3.7.2.3).

On the other hand, the localization in spots with a diameter of a few μm is a manifestation of specialty of nuclear reactions catalyzed by the trapped neutrons. Alien nuclei in the surface containing the cf-matter interact with trapped neutrons to induce reactions (2.1) – (2.3). Once a reaction occurs, the liberated energy is used to increase temperature of the site. The higher the temperature of the lattice, the easier the CFP occurs as many experimental data show (e.g. Celani et al. [1.29]). This process gives a positive feedback for the CFP resulting in the changes of the surface morphology observed very often as several examples are shown in Figs. 2.3, 2.5 and 2.12 in this paper.

The occurrence of positive feedback in the microscopic region resulting in changes of surface morphology might be an evidence for the macroscopic events observed several times in the process of CF investigation. This possibility had been pointed out in the papers presented at JCF8 [3.1] and ICCF14 [3.2].

The experimental data sets obtained in XLPE (cross-linked polyethylene) showing nuclear transmutations accompanied with water tree formation [3.3] explained by our model [3.4, 3.5] are another example of localization of nuclear reactions in the CFP even if the localization in this case is indirectly exhibited.

Using the experimental data sets introduced in Sections 2 and 3, we can contemplate applicability of the reactions (2.1) – (2.3) considered in the TNCF model.

The single neutron reaction (2.1) have been applied very widely to explain numerical relations between numbers of events N_x and N_y of events X and Y (X, Y: excess heat Q, nuclear transmutation NT, neutron n, triton t, helium 4 ($^4_2$He), - - -). Taking into further data obtained recently, we may conclude that the reaction (2.1) is applicable to the situation where the neutron density n_n assumed in the model is not too high ($n_n \leqq 10^9$ cm^{-3}). Main products of this mechanism are triton, excess heat, and nuclear products with small shift of mass numbers as many examples given in Section 2. (cf. [2.1] Tables 11.2 and 11.3 or [1.1] Tables 2.2 and 2.3)

The neutron-proton cluster reaction (2.2) have been applied to cases where occur nuclear transmutations with shifts of proton and mass numbers by more than two and four, respectively. Their examples are given in Subsection 2.7 and 2.8 in this paper. This reaction may be applicable to the situation where the neutron density n_n in the model is fairly high ($n_n \geq 10^9$ cm^{-3}).

The reaction (2.3) catalyzed by the neutron drop has been used to explain nuclear transmutations with enormous variety of product nuclides observed by Miley et al. [1.16, 1.17] and Mizuno et al. [1.9, 1.10] and Ohmori et al. [1.11, 1.12] in protium and deuterium systems. The situation where the reaction (2.3) occurs may be realized by formation of the cf-matter with a very high value of n_n ($n_n \geq 10^{10}$ cm^{-3}).

In these more than 20 years after the discovery of the cold fusion phenomenon [2.1], there have been elaborated various investigations cultivating new samples and applying new experimental techniques. As a result, we have wide view on the CFP in protium and deuterium systems; (1) localization of nuclear reactions producing tritium and nuclear transmutations at surface/boundary regions with a depth of about 1 μm and a width of about a few μm, (2) neutron emission with energies from about 3 to more than 10 MeV, (3) several laws or regularities of events in the CFP. These features of this phenomenon may be useful to accomplish the physics of the cold fusion phenomenon. We hope that the trial given in this paper serves as a useful step to the goal.

Acknowledgement

The author would like to express his thanks to Y. Iwamura for the paper [1.23] and

to F. Celani for the paper [1.29] making possible to use their detailed data in this paper.

References

1.1 H. Kozima, *The Science of the Cold Fusion Phenomenon*, Elsevier Science, 2006. ISBN-10: 0-08-045110-1.

1.2 J.R. Morrey, M.R. Caffee, H. Farrar, IV, N.J. Hoffman, G.B. Hudson, R.H. Jones, M.D. Kurz, J. Lupton, B.M. Oliver, B.V. Ruiz, J.F. Wacker and A. Van, "Measurements of Helium in Electrolyzed Palladium," *Fusion Technol*. **18**, 659 (1990).

1.3 P.K. Iyengar, "*Cold Fusion Results in BARC Experiments*" *Proc*. 5th *International Conf. on Emerging Nucl. Energy Systems*. (1989. Karlsruhe, Germany) p. 291 (1989). And also P. K. lyengar & M. Srinivasan (Eds), "BARC Studies in Cold Fusion (April-September 1989)" *Report BARC-1500*, (1989).

1.4 M. Srinivasan, A. Shyam, T.C. Kaushik, R.K. Rout, L.V. Kulkarni, M.S. Krishnan, S.K. Malhotra, V.G. Nagvenkar and P.K. Iyengar, "Observation of Tritium in Gas/ Plasma Loaded Titanium Samples," in *Anomalous Nuclear Effects in Deuterium /Solid Systems* (1990. Provo, Utah, USA), *AIP Conference Proceedings 228*. p. 514. American Institute of Physics, New York.

1.5 D.S. Silver, J. Dash and P.F. Keefe, "Surface Topography of a Palladium Cathode after Electrolysis in Heavy Water," *Fusion Technol*. **24**, pp. 423 – 430 (1993). And also J. Dash, G. Noble and D. Diman, "Changes in Surface Topography and Microcomposition of a Palladium Cathode caused by Electrolysis in Acidified Light Water" *Cold Fusion Sourcebook* (Minsk, Belarus, 1994), pp. 172 –180 (1994).

1.6 W.-S. Zhang and J. Dash, "Excess Heat Reproducibility and Evidence of Anomalous Elements after Electrolysis in $Pd/D_2O+H_2SO_4$ Electrolytic Cells," *Proc. ICCF13*, pp. 202 – 216 (2008).

1.7 M. Okamoto, H. Ogawa, Y. Yoshinaga, T. Kusunoki and O. Odawara, "Behavior of Key Elements in Pd for the Solid State Nuclear Phenomena Occurred in Heavy Water Electrolysis," *Proc. ICCF4* (Hawaii, USA, Dec. 6 — 9, 1993), Vol.3, p.14 (1994), EPRI, Palo Alto, California, USA.

1.7 J.O'M. Bockris and Z. Minevski, "Two Zones of 'Impurities' Observed after Prolonged Electrolysis of Deuterium on Palladium," *Infinite Energy*, **5 & 6**, 67 – 70 (1995 – 96).

1.9 T. Mizuno, T. Ohmori and M. Enyo, "Anomalous Isotopic Distribution in Palladium Cathode after Electrolysis," *J. New Energy* **1-2**, pp. 37 – 44 (1996)

1.10. T. Mizuno, T. Ohmori and M. Enyo, "Isotopic Changes of the Reaction Products induced by Cathodic Electrolysis in Pd," *J. New Energy* **1-3**, pp. 31 – 45 (1996)

1.11 T. Ohmori, T. Mizuno and M. Enyo, “Isotopic Distribution of Heavy Metal Elements Produced during the Light Water Electrolysis on Gold Electrode,” *J. New Energy* **1-3**, pp. 90 – 99 (1996)
1.12 T. Ohmori, T. Mizuno, Y. Nodasaka and M. Enyo, “Transmutation in a Gold-Light Water Electrolysis System,” *Fusion Technol.* **33**, pp. 367 – 382 (1998).
1.13 G.S. Qiao, X.M. Han, L.C. Kong and X.Z. Li, “Nuclear Transmutation in a Gas-Loading H/Pd System,” *J. New Energy,* **2-2**, pp. 48 – 52 (1997).
1.14 E. Campali, G. Fasano, S. Focardi, G. Lorusso, V. Gabbani, V. Montalbano, F. Piantelli, C. Stanghini, and S. Veronesi, “Photon and Particle Emission, Heat Production and Surface Transmutation in Ni-H System,” *Proc. ICCF11*, pp. 405 – 413 (2006).
1.15 E. Campali, S. Focardi, V. Gabbani, V. Montalbano, F. Piantelli, S. Veronesi and S. Veronesi, “Surface Analysis of Hydrogen-Loaded Nickel Alloys,” *Proc. ICCF11*, pp. 414 – 420 (2006).
1.16 G.H. Miley, G. Narne, M.J. Williams, J.A. Patterson, J. Nix, D. Cravens and H. Hora, “Quantitative Observation of Transmutation Products occurring in Thin-film coated Microspheres during Electrolysis,” *Proc. ICCF6* (1996, Hokkaido, Japan) pp. 629 – 644 (1996). And also
1.17 G.H. Miley and J.A. Patterson, “Nuclear Transmutations in Thin-film Nickel Coatings undergoing Electrolysis,” *J. New Energy* 1-3, pp. 5 – 34 (1996).
1.18 J. Patterson, “US Patent #5,607,563” *Elemental Energy* (*Cold Fusion*), 22, pp. 3 – 17 (1997).
1.19 Y. Iwamura, T. Itoh, N. Gotoh, M. Sakano and I. Toyoda, "Detection of Anomalous Elements, X-ray and Excess Heat induced by Continuous Diffusion of Deuterium through Multi-layer Cathode (Pd/CaO/Pd)," *Proc. ICCF7* (April 20 - 23, 1998, Vancouver, Canada), pp. 167 – 171 (1998). $^{57}Fe/^{56}Fe$ ratio increased largely.
1.20 Y. Iwamura, T. Itoh, M. Sakano and S. Sakai, “Observation of Low Energy Nuclear Reactions induced by D_2 Gas Permeation through Pd Complexes,” *Proc. ICCF9* (2002, Beijing, China) pp. 141 – 146 (2005).
1.21 Iwamura, T. Itoh, M. Sakano, S. Sakai and S. Kuribayashi, “Low Energy Nuclear Transmutation in Condensed Matter induced by D_2 Gas Permeation through Pd Complexes: Correlation between Deuterium Flux and Nuclear Products,” *Proc. ICCF10* (2003, Massachusetts, USA) pp. 435 – 446 (2006).
1.22 Y. Iwamura, T. Itoh, M. Sakano, N. Yamazaki, S. Kuribayashi, Y. Terada, T. Ishikawa and J. Kasagi, “Observation of Nuclear Transmutation Reactions induced by D_2 Gas Permeation through Pd Complexes” *Proc. ICCF11*, pp. 339 – 349 (2006)
1.23 Y. Iwamura, T. Itoh, M. Sakano, N. Yamazaki, S. Kuribayashi, Y. Terada and T.

Ishikawa, “Observation of Surface Distribution of Products by X-ray Fluorescence Spectrometry during D_2 Gas Permeation through Pd Complexes” *Proc. ICCF12* pp. 178 – 187 (2006).
1.24 H. Kozima, “The Cold Fusion Phenomenon as a Complexity (3) – Characteristics of the Complexity in the CFP –,” *Proc. JCF8*, pp. 85 – 91 (2007).
1.25 S. Szpak, P.A. Mosier-Boss, and M. H. Miles, “Calorimetry of the Pd + D Codeposition,” *Fusion. Technol*., **36** (1999) 234-241.
1.26 S. Szpak, P.A. Mosier–Boss, J. Dea and F. Gordon, “Polarized D+/Pd-D_2O System: Hot Spots and “Mini-Explosions,” *Proc. ICCF10*, pp. 13 – 22 (2006).
1.27 S. Szpak, P.A. Mosier-Boss, C. Young, F.E. Gordon, “The Effect of an External Electric Field on Surface Morphology of Co-deposited Pd/D Films” *J. Electroanal. Chem.* Pp. 284 – 290 (2005).
1.28 Szpak et al. “SPAWAR Systems Center-Pacific Pd:D Co-Deposition Research: Overview of Refereed LENR Publications,” *ICCF14* (2008), (to be published in 2010)
1.29 F. Celani, P. Marini, V. Di Stefano, M. Nakamura, O.M. Calamai, A. Spallone. A. Nuvoli, E. Purchi, V. Andreassi, B. Ortenzi, E. Righi, G. Trenta, A. Mancini, A. Takahashi and A. Kitamura, “First measurement on Nano-coated Ni Wire, at Very High Temperature, under He, Ar, H_2, D_2 Atmosphere and Their Mixtures,” Paper presented at 9th International Workshop on Anomalies in Hydrogen/Deuterium Loaded Metals (Sept. 17 – 19, 2010).
•
2.1 H. Kozima, *Discovery of the Cold Fusion Phenomenon* (Ohtake Shuppan Inc., 1998). ISBN 4-87186-044-2.
2.2 M. Fleischmann, S. Pons and M. Hawkins, "Electrochemically induced Nuclear Fusion of Deuterium," *J. Electroanal. Chem*., **261**, 301 – 308 (1989).
2.3 H. Kozima, “Quantum Physics of Cold Fusion Phenomenon,” *Developments in Quantum Physics Researches – 2004*, pp. 167 – 196, ed. V. Krasnoholovets, Nova Science Publishers, Inc., New York, 2004. ISBN 1-59454-003-9.
2.4 H. Kozima, J. Warner, C. Salas-Cano and J. Dash, “TNCF Model Explanation of Cold Fusion Phenomenon in Surface Layers of Cathodes in Electrolytic Experiments” *J. New Energy* **7-1**, pp. 81 – 95 (2003).
2.5 H. Kozima and F. Celani, “Brief Explanation of Experimental Data Set of Excess Heat and Nuclear Transmutation in Multiply Nanocoated Ni Wire,” *Proc. JCF11* (in this issue).
2.6 H. Kozima, K. Yoshimoto, H. Kudoh, M. Fujii and M. Ohta, “Analysis of Zn and Excess Heat Generation in Pd/H_2 (D_2) System by TNCF Model,” *J. New Energy* **6-3**,

pp.97 – 102 (2002)
2.7 F. Celani, A. Spallone, T. Toripodi, D. Di Giacchino, P. Marini, V. Di Stefano, A. Mancini and S. Pace, “New Kinds of Electrolytic Regimes and Geometrical Configurations to Obtain Anomalous Results in Pd(M)-D Systems,” *Proc. ICCF6*, pp. 93 – 104 (1996).
2.8 H. Kozima, “Neutron Emission in the Cold Fusion Phenomenon,” *Proc. JCF11* (in this issue).
2.9 S. Focardi, R. Habel and F. Piontelli, ”Anomalous Heat Production in Ni-H System,” *Nuovo Cimento*, **107A**, 163 (1994).
2.10 E.G. Campari, S. Focardi, V. Gabbani, V. Montalbano, F. Piantelli, E. Porcu, E. Tosti and S. Veronesi, ”Ni-H System,” *Proc. ICCF8* pp. 69 - 74 (2000).

3.1 H. Kozima, “The Cold Fusion Phenomenon as a Complexity (3) – Characteristics of the Complexity in the CFP –, “*Proc. JCF 8*, pp. 85 – 91 (2007).
3.2 H. Kozima, “Complexity in the Cold Fusion Phenomenon,**”** *Proc. ICCF14* (August 10 – 15, 2008, Washington D.C., USA), Eds. J. Nagel and M.E. Melich, pp. 613 – 617 (2010).
3.3 T. Kumazawa, W. Nakagawa and H. Tsurumaru, “A Study on Behavior of Inorganic Impurities in Water Tree,” *Electrical Engineering in Japan* **153**, 1 – 13 (2005).
3.4 H. Kozima, “An Explanation of Nuclear Transmutation in XLPE (Crosslinked Polyethylene) Films with and without Water Trees,” *Proc. JCF8*, pp. 44 – 50 (2007).
3.5. H. Kozima and H. Date, “Nuclear Transmutations in Polyethylene (XLPE) Films and Water Tree Generation in Them,” *Proc. ICCF14*, pp. 618 – 622 (2010).